Chapter 18
Petrophysical Characterization of Sandstone Reservoir from Well Log Data: A Case Study from South Tapti Formation, India

N. P. Singh, S. P. Maurya and Kumar Hemant Singh

Abstract   The present study is aimed at evaluating the reservoir potentials of South Tapti Basin of India with limitation to the available data. A number of petrophysical parameters, i.e., effective porosity (Φ), water saturation (S_w), formation water resistivity (R_w), hydrocarbon saturation (S_o), and true resistivity (R_t), are evaluated using the well log data, and the reservoir characterization is performed. The analysis shows a hydrocarbon-bearing zone in between 1866 and 1874 m, which contains gamma ray (GR) value of 34.4 API, resistivity of 117.3 Ω m, and average porosity of 35.7%. To know the fluid type in the reservoir zone, neutron porosity and density porosity are plotted together and a crossover has been noticed at 1866–1874 m depth which indicates that the reservoir is filled with gas. The analysis of petrophysical parameters and cross-plots shows that the reservoir is filled with sandstone with some clay content separated by shale markers, which act as seal rock for the reservoir.

Keywords Petrophysical characterization · South Tapti Basin · Sandstone reservoir · Cross-plots · Hydrocarbon saturation

1   Introduction

Well logs have been successfully used in exploration and development wells and are routinely used to quantify depth and thickness of productive zones (Adeoti et al. 2009; Maurya and Singh 2015). Schlumberger brothers in Alsace, France, first introduced geophysical well logging technique in 1927. Logging is carried out by physical measurements (sonde) made by instruments lowered into the hole (geophysical logs) and supported by laboratory experiments on core samples (Ofwona 2014). Immediately after the well is drilled, the formations are exposed to well-bore and this is

N. P. Singh · S. P. Maurya (✉)
Department of Geophysics, Institute of Science, Banaras Hindu University, Varanasi 221005, India
e-mail: spm.iitb@gmail.com

K. H. Singh
Department of Earth Sciences, Indian Institute of Technology, Bombay, Maharashtra 400076, India

the best time to determine the properties of rocks in the vicinity of borehole using open-hole logging tools. In wells with complex trajectories, logging tools are used as part of drilling tool assembly. This approach is termed as logging while drilling (LWD) (Economides and Nolte 1989). Important logs include temperature, pressure, gamma, neutron, caliper log, and resistivity. The main objective of petrophysical well log analysis is to transform well log measurements into reservoir properties like permeability, porosity, oil saturation, water saturation, mineralogy, etc. The proposed study aims at interpretation of well log data and quantitative evaluation of petrophysical properties such as water saturation in parts of South Tapti Basin.

The South Tapti field covers an approximately area of 570 square miles and lies approximately 100 miles north-northwest of Mumbai City, India. In this paper, well log analysis is performed on the logs obtained from wells comprising the clastic sediments of late Oligocene Daman formation in South Tapti Field (Wandrey 2004; Saha et al. 2009). The quality of reservoir in terms of parameters like shale volume, effective porosity, water and hydrocarbon saturation, and permeability are evaluated, and the results are discussed.

2 Methodology

The well log data from the South Tapti Field is made available for research and development by BG, India. An essential step in formation evaluation process is the determination of amount of shale present in the formation (Opuwari 2010; Adaeze et al. 2012). This helps to calculate the correct formation porosity and fluid content within the pay zone. Volume of shale is calculated following the integrated approach by utilizing the gamma ray log, SP log, neutron–density log, and resistivity log data (Adeoti et al. 2009). Porosity is also calculated from density log. From the qualitative observation of log plots, the crossover in neutron–density log, low intensity value of natural gamma ray log, separation in shallow and deep resistivity log values, suppression in SP log and higher value in sonic log suggested the presence of hydrocarbons between 1866 and 1874 m depth in the study area.

The analysis is performed in the depth range of 1830–1930 m as the reservoir zone is expected within this interval. Water saturation is calculated using Archie's equation. The other important petrophysical parameters, i.e., permeability, are calculated using the Timur equation in which irreducible water saturation is calculated from the bulk volume water (BVW). The bulk volume water is calculated at several depths within the reservoir zones. A constant or near constant values indicate a single rock-type bearing zone at irreducible water saturation. When a zone is at irreducible water saturation, water in the uninvaded zone (S_w) does not move as it is held on grains by capillary pressure.

3   Petrophysical Evaluation

The log data from South Tapti Formation is evaluated, and the derived petrophysical parameters along with other logs are shown in Fig. 1. The figure shows the natural gamma ray (GR), resistivity (R_t/R_{xo}), porosity (PhiD/Nphi), shale volume (VshND/VshGR), and effective porosity (PhiE) log calculated from the well log data. The analyses of log data show interesting features between depth interval 1866–1874 m. The natural gamma ray values are very low, the flushed zone and the invaded zone resistivity is very high, and there is marked crossover when the density and the neutron porosity logs are plotted together. Within the same interval, the shale volume calculated from gamma ray log and neutron log shows a low value, while the estimated effective porosity is very high. This analysis suggests that this could be a prospective hydrocarbon-bearing zone which needs further detailed analysis for its characterization.

Cross-plots are charts based on the slope and intercept of two porosity log responses (depending on matrix lithology, and pore fluid). The cross-plots of bulk density against P-impedance and lambda-rho against Poisson's ratio are generated for the depth interval 1830–1930 m (Fig. 2a). The cross-plot in Fig. 2a shows concentration of low bulk density and P-impedance values indicating prospective reservoir zone between 1866 and 1874 m. This low value indicates the presence of hydrocarbon
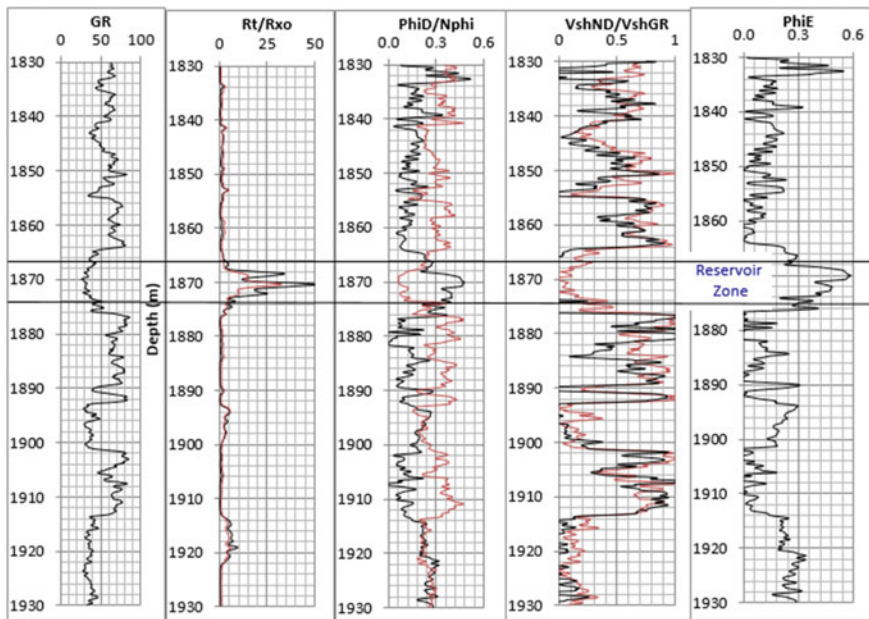
Fig. 1   Gamma ray, resistivity log, porosity log, shale volume, and effective porosity log calculated from well log data
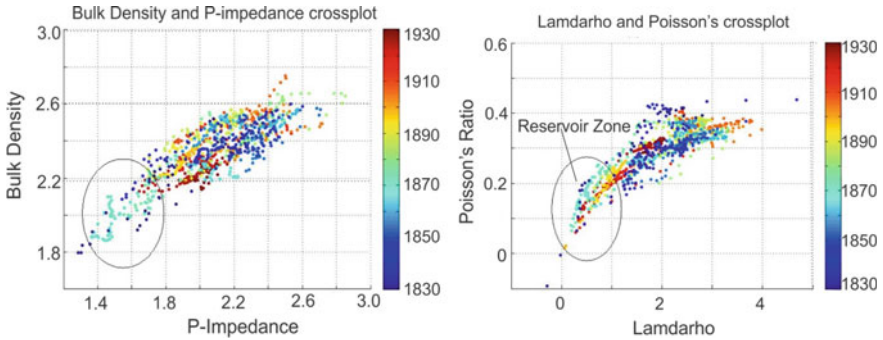
Fig. 2 Cross-plot between **a** the bulk density and the P-impedance and Poisson's ratio and **b** the Lambda-rho cross-plot. The color bar indicates depth

in this zone. The cross-plot between Lambda-rho and Poisson's ratio shows a similar concentration of low values within the zone between 1866 and 1874 m (Fig. 2b). The cross-plots in Fig. 2a, b suggest that this zone is possibly hydrocarbon bearing and reiterates the qualitative analysis of gamma ray, neutron and density porosity, and resistivity logs.

4 Lithology Identification

An interpretation of lithology is performed through a systematic approach. The gross lithology is collaborated and compared at the same depth, horizontally, to the gamma ray log. Cross-plots are prepared for classification of sandstone, limestone, and dolomite lithologies. When data points from lithology are plotted, they fall on the charts lithology lines.

When combinations of those lithologies are present, the points mostly fall between the lines. The porosity is determined by joining the data points and constructing a porosity scale between major lithologies (Rider 2000).

4.1 Neutron–Density Cross-Plot

One of the methods available for porosity log analysis involves the density–neutron cross-plot. A cross-plot method, called the shaly sand model, is widely used. However, this model is considered to be a poor model for any sandstone that contains other minerals in addition to quartz. The complex lithology model works well in quartz sands and is a preferred model for analysis (Adaeze et al. 2012).

Neutron–density cross-plot shows scattered data distributed on the entire line (dolomite, limestone, and sandstone) suggesting the presence of these three minerals
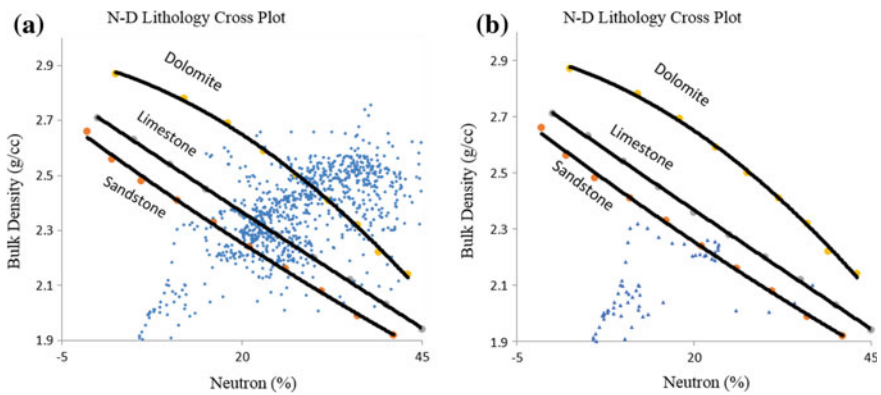
Fig. 3 Bulk-density versus neutron–density cross-plot **a** for depth 1830–1930 m, **b** for reservoir zone (1866–1974 m)

between 1830 and 1930 m (Fig. 3a). The neutron and density porosity cross-plot for reservoir zone (depth 1866–1874 m) is shown in Fig. 3b. The figure shows that almost all plots lie on or below the sandstone line shows the rock type dominated by sandstone in the reservoir zone with some level of limestone.
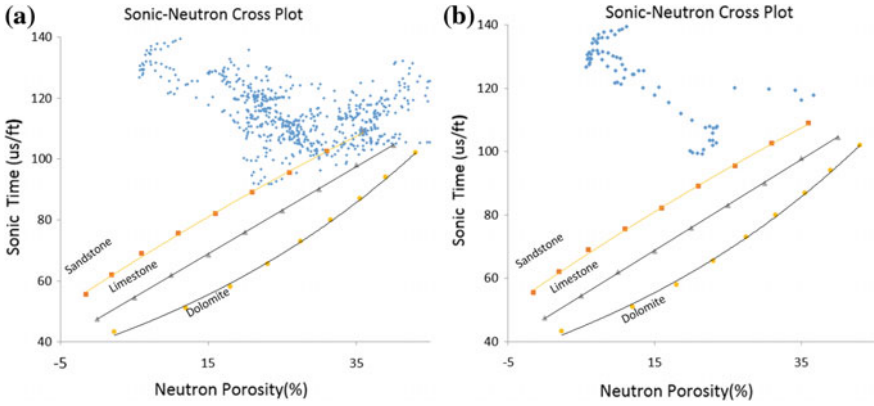
4.2   Sonic–Neutron Cross-Plot

The sonic–neutron cross-plot method involves the simultaneous solution of the sonic and neutron response equations for porosity. Complex lithology is best suited to this method. Since both logs respond to shale, the formulae do not work in shaly sands with same accuracy (Crain 2002).

   The sonic–neutron cross-plot shows the scatter of points spreading across all three rock types (sandstone, limestone, and dolomite) but mostly lies between sandstone and limestone (Fig. 4a). The figure suggests that a mixture of sandstone, limestone, and dolomite in small quantity is present between depth intervals 1830 and 1930 m. Figure 4b shows the cross-plot in the depth range of reservoir (1866–1877 m) which shows data lying along the sandstone line or above it. This figure indicates that the reservoir zone is dominated by sandstone rock types.
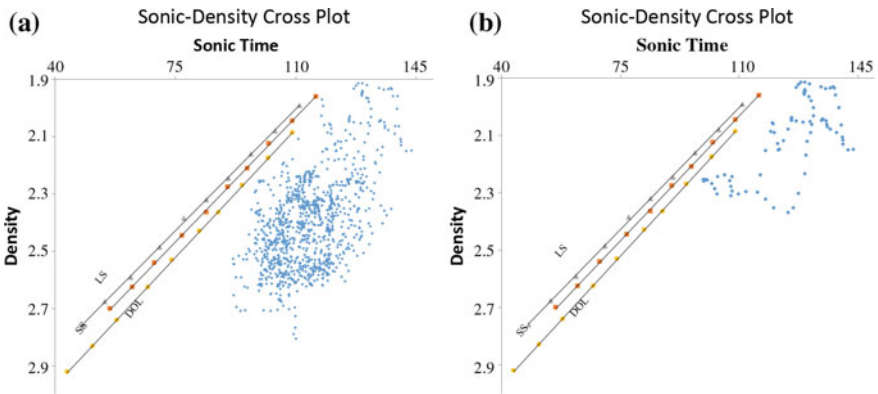
4.3   Sonic–Density Cross-Plot

The sonic–density cross-plot method involves a simultaneous solution of the sonic and density response equations for porosity. The sonic–density cross-plot works

Fig. 4 Sonic time versus neutron porosity cross-plot **a** for depth 1830–1930 m, **b** for reservoir zone (1866–1877 m)

ideally in shaly sands with no gas. The resolution is poor in carbonates, and the presence of gas makes the result too high (Rider 2000).

The sonic–density cross-plot in Fig. 5a shows the scatter of plotted points inclined toward dolomite line indicating the presence of dolomite in the formation. The sonic–density cross-plot for reservoir depth also shows a similar response suggesting the dominance of dolomite in the reservoir zone (Fig. 5b). The cross-plot does not appear to be accurately predicting the lithology compared to other cross-plots (Figs. 3 and 4) because the distance between the sandstone, limestone, and dolomite line is too small to reliably predict the lithology. Thus, the cross-plot in Fig. 5 is not reliable and not considered for our analysis.

Fig. 5 Sonic time versus density porosity cross-plot **a** for depth 1830–1930 m, **b** for reservoir zone (1866–1877 m)

Fig. 6 Bulk-volume-water cross-plot (Swa vs. PhiND)
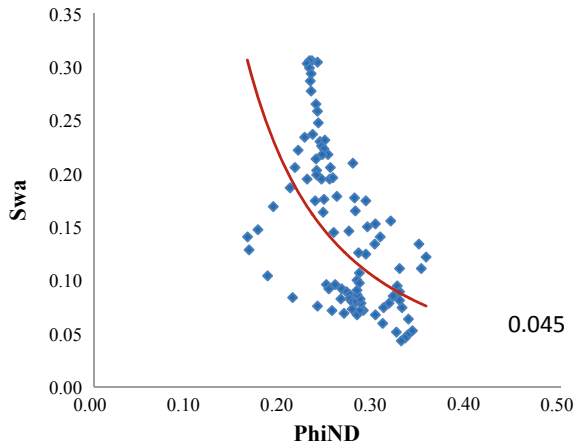
4.4 Bulk Volume Water

The product of a formation's water saturation (S_w) and its porosity is the bulk volume water (BVW) , $BVW = S_w * \emptyset$. If values for bulk volume water calculated at several depths in a formation are constant or very close to constant, they indicate that the zone is of a single rock type with irreducible water saturation (S_{wirr}). When a zone has irreducible water saturation, water in the uninvaded zone (S_w) does not move because it is held on grains by capillary pressure. Therefore, hydrocarbon production from a zone at irreducible water saturation should be water-free (Morris and Biggs 1967).

The Buckles plot (Asquith et al. 2004) is a graph of porosity (φ) versus S_w. Points of equal *BVW* form hyperbolic curves across this plot. If *BVW* is plotted using data from a formation at irreducible water saturation, the points fall along a single hyperbolic curve. If the data come from reservoirs with higher percentages of produced water, the points are more scattered. For the reservoir zone (1865–1875 m), the Buckles plot shows saturation value of 0.045. So, it is irreducible water. Figure 6 shows the plot of bulk volume water.

4.5 Residual Oil Saturation (ROS)

ROS is the saturation value of the oil that remains after a displacing process of crude oil system by water or gas injection. Residual oil saturation is oil saturation that cannot be produced from an oil reservoir from gas or water displacement. It is usually considered the immobile oil saturation after conventional (gas or water displacement) (Crain 2002).

ROS is given by:

$$ROS = 1 - S_{xo} \qquad (1)$$

where S_{xo} is water saturation in flushed zone.

4.5.1 Movable Oil Saturation (MOS)

It is important to recognize that only a fraction of oil in place is ultimately produced in most reservoirs. This poses a challenge to attain better recovery, requiring a thorough understanding of reservoir behavior (Waldschmidt et al. 1956). This necessitates the estimation of movable oil saturation, which represents the maximum volume of oil that can be moved or produced. Hence, the movable oil saturation is defined as:

Movable oil saturation = initial oil saturation − residual oil saturation

$$MOS = S_{xo} - S_{w} \qquad (2)$$

where S_{w} is water saturation and S_{xo} is saturation in flushed zone (Asquith et al. 2004).

4.6 Movable Hydrocarbon Index (MHI)

The movable hydrocarbon index is given by

$$MHI = \frac{S_{w}}{S_{xo}} \qquad (3)$$

Water saturation of the flushed zone (S_{xo}) can be used as an indicator of hydrocarbon moveability. If the value of S_{xo} is much larger than S_{w}, then hydrocarbons in the flushed zone have probably been moved or flushed out of the zone nearest the borehole by the invading drilling fluids (R_{mf}). If the ratio S_{w}/S_{xo} is equal to or greater than 1.0, then hydrocarbons were not moved during invasion. This is true regardless of whether or not a formation contains hydrocarbons. Whenever the ratio S_{w}/S_{xo} is less than 0.7 for sandstones or less than 0.6 for carbonates, moveable hydrocarbons are indicated (Schlumberger 1991).

The computed bulk volume water, residual oil saturation, moveable oil saturation, and moveable hydrocarbon index are given in Table 1 along with the depth, porosity estimated from neutron (NPHI) and density (PHID) log and water saturation for reservoir zone only. Table 2 contains the estimated lithology from cross-plots with PEF-derived lithology, volume of shale, and porosity estimated from density log (PhiD) for a depth range of 1854–1874 m.

Table 1 Reservoir properties estimated for depth from 1866 to 1874 m (reservoir zone)

DEPTH	NPHI	PHID	SW	BVW	ROS	MOS	MHI
1866.0	0.24	0.25	0.24	0.06	−0.14	0.89	0.21
1866.5	0.23	0.28	0.18	0.05	0.06	0.77	0.19
1867.0	0.22	0.27	0.20	0.05	0.09	0.71	0.22
1867.5	0.20	0.24	0.21	0.05	0.12	0.67	0.24
1868.0	0.12	0.20	0.12	0.02	0.23	0.65	0.15
1868.5	0.09	0.35	0.05	0.02	0.62	0.33	0.14
1869.0	0.06	0.44	0.05	0.02	0.64	0.30	0.15
1869.5	0.06	0.46	0.07	0.03	0.60	0.33	0.17
1870.0	0.06	0.48	0.04	0.02	0.71	0.25	0.13
1870.5	0.07	0.46	0.03	0.02	0.81	0.15	0.17
1871.0	0.12	0.39	0.05	0.02	0.51	0.43	0.11
1871.5	0.11	0.36	0.07	0.02	0.48	0.45	0.13
1872.0	0.07	0.39	0.05	0.02	0.57	0.37	0.13
1872.5	0.08	0.39	0.07	0.03	0.57	0.35	0.17
1873.0	0.12	0.38	0.12	0.05	0.50	0.38	0.25
1873.5	0.16	0.37	0.10	0.04	0.54	0.36	0.21
1874.0	0.35	0.28	0.17	0.05	0.37	0.46	0.28

5   Determination of Cutoff and Net Pay

The final aim of any petrophysical analysis is to find net pay thickness with proper petrophysical cutoffs. Net pay determination usually involves defining threshold values (or cutoffs) of the characteristics of interest. These limiting values are designed to define those rock volumes that are not likely to contribute significantly to the hydrocarbon production. The starting point in determining cutoff is to identify reference parameter that allows us to distinguish between intervals that have reservoir potential and intervals that do not. There is no single applicable approach to the identification of cutoff (Worthington and Cosentino 2005).

There are several techniques or criteria to define cutoffs; clean rocks with low volume of shales Vsh usually have few problems and have capability to store hydrocarbons (Hamada 1996). As a rock becomes shalier, it becomes a poor reservoir rock. There is a point of Vsh beyond which there are no more significant contribution to store hydrocarbons. That point could be taken as Vsh cutoff for pay rocks. The same concept applies for total porosity ϕ_t.

Table 2 Predicted lithology on the basis of PE factor and cross-plots

DEPTH (m)	PEF	Vshale (%)	PhiD (%)	Lithology (On the basis of PEF)	Lithology (On the basis of xplot)
1850.0–1850.1	2.9	63	7	Sandy shale	Dolomite + limestone + sandstone
1850.2–1851.1	3.6	84	9	Compact shale	Dolomite + limestone + sandstone
1851.2–1852.5	2.7	58	18	Sand + shale (18% Phi)	Dolomite + limestone + sandstone
1852.6–1853.3	3.4	45	9	Compact shale	Dolomite + limestone + sandstone
1853.4–1854.6	2.4	25	19	Sand + dolomite	Dolomite + limestone + sandstone
1854.7–1855.1	1.8	44	16	Sand with water (16% Phi)	Dolomite + limestone + sandstone
1855.2–1855.3	2.4	68	10	Sandy shale	Dolomite + limestone
1855.4–1855.5	3.4	70	13	Shale	Dolomite + limestone
1855.6–1855.8	4.1	77	17	Shale + limestone(17% Phi)	Dolomite + limestone
1855.9–1856.4	3.5	87	9	Shale	Dolomite + limestone
1856.5–1857.0	3.9	83	11	Compact shale	Dolomite + limestone
1857.1–1858.7	2.6	73	12	Sandy shale	Dolomite + limestone
1858.8–1859.4	2.2	62	14	Sand + uncompact shale	Dolomite + limestone
1859.5–1859.7	2.9	73	12	Uncompact sandy shale	Dolomite + limestone
1859.8–1860.0	3.7	84	9	Compact shale	Dolomite + limestone
1860.1–1860.7	4.5	68	9	Halite + shale	Dolomite + limestone
1860.8–1860.8	3.7	73	5	Compact shale	Dolomite + limestone
1860.9–1862.1	3.1	66	8	Sandy shale	Dolomite + limestone
1862.2–1862.3	3.8	69	10	Compact shale	Dolomite + limestone
1862.4–1863.8	4.3	89	8	Shale + limestone	Dolomite + limestone
1863.9–1864.1	3.4	86	9	Shale	Dolomite + limestone

(continued)

Table 2 (continued)

DEPTH (m)	PEF	Vshale (%)	PhiD (%)	Lithology (On the basis of PEF)	Lithology (On the basis of xplot)
1864.2–1864.2	2.5	67	11	Sand + shale	Dolomite + limestone
1864.3–1865.6	2.0	15	33	Sand with water (33% Phi)	Dolomite + limestone
1865.7–1866.0	2.2	19	24	Sandstone	Dolomite + limestone
1866.1–1866.2	2.0	14	26	Sandstone	Sandstone
1866.3–1869.5	2.1	15	31	Sandstone with gas (31% Phi)	Sandstone
1869.6–1869.9	1.8	9	40	Sandstone with water (40% Phi)	Sandstone
1874.0–1874.0	2.7	42	28	Dolomite + sand	Dolomite + limestone + sandstone
1874.1–1874.6	3.3	29	27	Dolomite + sand	Dolomite + limestone + sandstone

5.1 Determination of Petrophysical Cutoff

Net pay is defined as the thickness of rock that contributes to economically viable production with today's technology, today's prices, and today's costs. Net pay is obviously a moving target since technology, prices, and costs vary almost daily.

Tight reservoirs or shaly zones that were bypassed in the past are now prospective pay zones due to new technology and continued demand for hydrocarbons. We determine net pay by applying appropriate cutoffs to reservoir properties so that unproductive or uneconomic layers are not counted. This can be done with both log and core data (if available).

Cumulative reservoir properties, after appropriate cutoffs are applied, provide information about the pore volume (PV), hydrocarbon pore volume (HPV), and flow capacity (KH) of a potential pay zone. These values are used to calculate hydrocarbon in place, recoverable reserves, and productivity of wells. The following algorithm is a highly simplified one-pass approach, which would need considerable adjustment to run on a real computer. However, it is suitable for discussion purposes (Guo 2004).

It is normal to apply cutoffs to each calculated result to eliminate poor quality or unproductive zones. Cutoffs are usually applied to shale volume, porosity, water saturation, and permeability. The layer is not counted as "pay" if it fails any one of the four cutoffs. Typical cutoffs are:

$$IF(VSH_{max} \leq SH_{max}) * (PHI_e \geq PHI_{min}) * (S_w \leq SW_{max}) = 1 \qquad (5)$$

$$THEN\ PAYFLAG = 1$$

$$ELSE\ PAYFLAG = 0$$

$$H_{net} = SUM(PAYFLAG * INCR) \qquad (6)$$

where:

H_{net} = net pay
INCR = digitizing increment
PHI_{min} = porosity cutoff (fractional)
PHI_e = effective porosity (fractional)
S_w = water saturation (fractional)
SW_{max} = saturation cutoff (fractional)
VSH = volume of shale (fractional)
VSH_{max} = shale volume cutoff (fractional).

Typically:

VSH_{max} = 0.25–0.45
PHI_{min} = 0.03–0.16
SW_{max} = 0.30–0.70.

These values must be appropriate for the rock sequence. Values in unconventional reservoirs may be more extreme. In reservoir simulation work, the net reservoir is also needed. In this case, set $SW_{max} = 1.00$ (Guo 2004). The effective porosity, water saturation, reservoir, and net pay zone are shown in Fig. 7. Table 3 describes the numerical values of the net pay estimation. The pay thickness is estimated to be 10.8 m, whereas residual and non-residual thicknesses are estimated to be 12 m and 1 m, respectively.
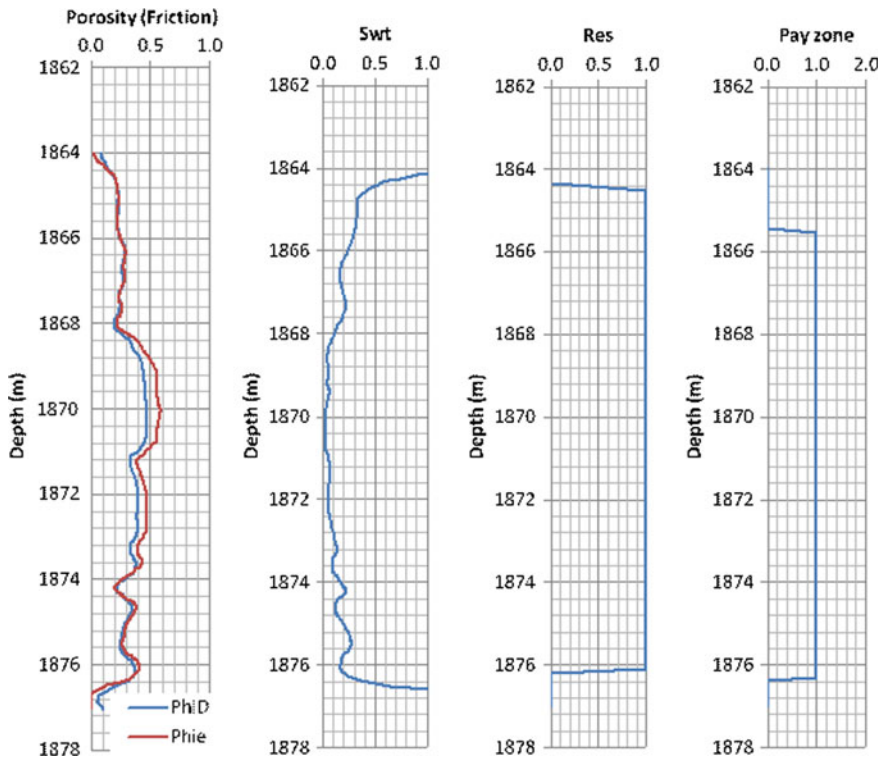

Fig. 7 Porosity, water saturation, reservoir, and net pay zone (left to right) of the area

Table 3 Net pay estimation of the South Tapti basin

Top (m)	Bottom (m)	Interval (m)	Pay (m)	Res	Non-res	Total thickness (m)
1864	1877	13	10.8	12	1	13

6 Conclusions

1. The volume of shale is calculated using gamma ray and neutron–density log which shows a trend without much variation till 1865 m before it shows a marked decrease in volume until a depth of 1876 m. The volume of shale decreases again between 1914 and 1930 m depth.
2. The depth interval between 1866 and 1874 m witnesses the neutron and the density porosity crossover indicating the presence of a gas zone. The gamma ray count is also low in this zone. The average porosity however is high (30–45)%. This suggests along with the cross-plot results that the reservoir is sandstone with high porosity between 1866 and 1874 m.
3. The water saturation is very low in the reservoir zone, and resistivity curve in deep region (R_t) is high concurring with our inference for the presence of a gas zone.
4. The lithology is predicted using different cross-plots like neutron–density, sonic–neutron, and sonic–density which also indicates the presence of sandstone reservoir at (1866–1874) m and limestone at (1841–1845) m and (1900–1915) m.
5. The flushed zone water saturation is found using resistivity of mud filtrate and resistivity of flushed zone. Residual oil saturation(ROS) , movable oil saturation (MOS), and movable hydrocarbon index (MHI) are found, and it is observed that hydrocarbons are movable as MHI < 0.7.
6. Reservoir and pay zone analysis is performed, and it is found that the reservoir is 12 m thick and pay zone is 10.8 m thick which makes it a good reservoir.

References

Adaeze IU, Samuel OO, Cajetan JI (2012) Petrophysical evaluation of Uzek well using well log and core data, Offshore Depobelt, Niger Delta, Nigeria. Adv Appl Sci Res 3(5):2966–2991

Adeoti L, Ayolabi EA, James PL (2009) An integrated approach to volume of shale analysis: Niger Delta example, Offrire Field. World Appl Sci J 7(4):448–452

Asquith GB, Krygowski D, Gibson CR (2004) Basic well log analysis, vol 16. American Association of Petroleum Geologists, Tulsa, TX, USA

Crain ER (2002) Crain's petrophysical handbook. Spectrum 2000 Mindware Ltd., Alberta, Canada

Economides MJ, Nolte KG (1989) Reservoir stimulation, vol 2. Englewood Cliffs, Prentice Hall, NJ, USA

Guo R (2004) Supplement to determining method of cut-off value of net pay. Petroleum Exploration and Development. http://en.cnki.com.cn/Article_en/CJFDTOTAL-SKYK200405044.htm. Accessed 22 Mar 2019

Hamada GM (1996) An integrated approach to determine shale volume and hydrocarbon potential in shaly sand. In: SCA international symposium. http://www.jgmaas.com/SCA/1996/SCA1996-41.pdf. Accessed 21 Mar 2019

Maurya SP, Singh KH (2015) LP and ML sparse spike inversion for reservoir characterization—a case study from Blackfoot area, Alberta, Canada. In: 77th EAGE conference and exhibition. https://doi.org/10.3997/2214-4609.201412822

Morris RL, Biggs WP (1967) Using log-derived values of water saturation and porosity. In: Society of petrophysicists and well-log analysts, 8th annual logging symposium, Denver, CO, USA, 12–14 June

Ofwona CO (2014) Introduction to geophysical well logging and flow testing. Short Course V on Exploration for Geothermal Resources. https://orkustofnun.is/gogn/unu-gtp-sc/UNU-GTP-SC-11-35.pdf. Accessed 22 Mar 2019

Opuwari M (2010) Petrophysical evaluation of the Albian age gas bearing sandstone reservoirs of the OM field, Orange basin, South Africa. Ph.D. dissertation, University of the Western Cape. https://core.ac.uk/download/pdf/58914267.pdf. Accessed 22 Mar 2019

Rider MH (2000) The geological interpretation of well logs, 2nd edn. Whittles Publishing, Caithness, UK

Saha S, Stuart DB, Stuart G, Thurlow A, Andy T (2009) The stratigraphic and sedimen-tological evolution of the Mahim, Daman and Mahuva formation reservoirs of the Tapti fields: tidally-influenced deposition in an Oligo-Miocene tropical estuarine embayment on the continental shelf of Western India. In: AAPG Hedberg conference, Jakarta, Indone-sia. http://www.searchanddiscovery.com/pdfz/abstracts/pdf/2010/hedberg_indonesia/abstracts/ndx_saha.pdf.html. Accessed 22 Mar 2019

Schlumberger (1991) Log interpretation principles/applications. Schlumberger Educational Ser-vices. https://www.slb.com/resources/publications/books/lipa.aspx. Accessed 21 Mar 2019

Waldschmidt WA, Fitzgerald PE, Lunsford CL (1956) Classification of porosity and fractures in reservoir rocks. Am Assoc Petrol Geol Bull 40:953–974

Wandrey C (2004) Bombay geologic province eocene to miocene composite total petroleum system, India. U.S. Geological Survey Bulletin 2208-F. https://pubs.usgs.gov/bul/2208/F/b2208-f.pdf. Accessed 17 Mar 2019

Worthington PF, Cosentino L (2005) The role of cut-offs in integrated reservoir studies. SPEREE 8(4):276–290. https://doi.org/10.2118/84387-PA